JOURNAL OF
Optical Communications
and Networking

100 Gb/s/λ polarization multiplexing PON downlink based on simplified heterodyne coherent reception

David Izquierdo,[1,*] Miguel Barrio,[1] Pascual Sevillano,[1] Jose A. Altabas,[2] and Ignacio Garces[1]

[1]Aragon Institute for Engineering Research (I3A), Universidad de Zaragoza, Zaragoza, Spain
[2]Bifrost Communications, Lyngby, Denmark
*d.izquierdo@unizar.es

Received 21 May 2024; revised 27 October 2024; accepted 30 October 2024; published 26 November 2024

In this work, we experimentally demonstrate a 100 Gb/s/λ downstream transmission link for coherent passive optical networks (PONs) up to 50 km, achieving an optical power budget of 29 dB through polarization multiplexing (PolMux) of two 50 Gb/s channels using multiband carrierless amplitude phase modulation (multiCAP) and optical single side band (OSSB) modulation. Additionally, we introduce a separate PolMux 50 Gb/s link that presents an optical power budget of 38.7 dB. Both links have been achieved using a simplified polarization-demultiplexing heterodyne coherent receiver. The robustness of the system is experimentally evaluated by analyzing its response to various input states of polarization. The transmission has been accomplished using 10 GHz electrical bandwidth devices at both the transmission and receiving ends, thereby paving the way for low-cost 100G links suitable for applications such as PONs.

https://doi.org/10.1364/JOCN.530478

1. INTRODUCTION

Optical access networks currently serve as the cornerstone for home and office broadband communications, offering standard client bitrates of 10 Gb/s. However, the increasing demand for higher bitrates has driven extensive research aimed at implementing 50 Gb/s and 100 Gb/s single-wavelength links in next generation passive optical networks and 5/6G fronthaul communications [1–3]. Increasing the bitrate typically requires enhancement in the electronics and opto-electronics bandwidth capabilities of the transmitter and receivers, often employing multilevel modulation formats. Several techniques have been explored to achieve single-polarization 50 Gb/s links using 25 GHz or 10 GHz bandwidth components and intensity modulation/direct detection (IM/DD) schemes. Some solutions rely on 4-level pulse amplitude modulation (PAM4) [4,5], which provides a straightforward solution by doubling the bit count; while others employ orthogonal frequency division multiplexing (OFDM), discrete multitone (DMT), or multiband carrierless amplitude phase (multiCAP) modulation schemes [6]. These techniques exploit their bit and power loading capabilities to further increase the bit count per Hz, especially in the O-band where dispersion is minimal [7]. However, these high bandwidth, non-coherent solutions exhibit poor sensitivities at the receiver, requiring higher launch power to achieve adequate optical power budgets. This requirement often leads to problems arising from strong fiber non-linear effects. Additionally, these systems are affected by chromatic dispersion (CD) issues, the severity of which escalates with bandwidth. Furthermore, these systems depend on intensive digital signal processing (DSP) algorithms to mitigate the aforementioned effects and typically require the inclusion of an optical pre-amplifier at the receiver end. Given these limitations, IM/DD systems are approaching their operational limit at 100 Gb/s. Consequently, coherent schemes are expected to replace IM/DD systems for capacities exceeding this threshold [8]. Thus, it is crucial to experimentally assess the performance of such systems, which will be the foundation for future >100 Gb/s/λ links, a capacity unachievable with existing IM/DD technology [9].

Coherent and quasi-coherent optical receivers are receiving significant interest for access links, as they can achieve substantial optical power budgets with moderate input optical powers [10]. These systems effectively filter most of the optical noise outside the signal bandwidth and completely mitigate fading issues through DSP-based compensation of the CD of the fiber. However, these receivers exhibit polarization dependency, require an additional laser that operates as a local oscillator (LO), and generally demand strong DSP for signal retrieval. Notably, while quasi-coherent schemes do not require DSP,

they cannot dynamically compensate the CD of the channel. Among these challenges, the polarization dependence of the coherent received signal poses a significant issue, as there is currently no technical solution to avoid the continuous fluctuation of the signal state of polarization over time, resulting in received signal instability. For intradyne standard coherent receivers, the integration of two 90° hybrids not only makes the signal independent of the polarization but also serves as an architecture for polarization multiplexing (PolMux) transmission. Historically, heterodyne solutions have been used for access networks due to their simpler and more cost-effective receiver designs [11], despite their needs of higher bandwidth. Additionally, several approaches to mitigate polarization dependence have been proposed. Notably, architectures similar to the Glance polarization independent coherent receiver [12] have received considerable attention [13,14]. In previous research [15], we used this architecture to achieve a 50 Gb/s polarization-insensitive response over a 50 km link based on the multiCAP modulated signal, where optical single sideband (OSSB) modulation was used to fit the signal to 10 GHz bandwidth opto-electronics. Despite the recent trends of optical receivers with bandwidths exceeding 20 GHz, we remain confident that the use of 10 GHz bandwidth devices will prove advantageous in delivering a cost-effective solution for coherent access. In [16], the same receiver architecture supported a PolMux transmission by manually controlling the state of polarization of the incoming signal and effectively doubling the bitrate up to 100 Gb/s with an optical power budget of 21 dB. The primary challenge involved recovering the two channels in a heterodyne configuration, requiring the use of two different phase-locked loops (PLLs) and precise alignment for adequate recovery. In [17] we proved the feasibility of receiving mixed PolMux channels and successfully recovering them using post-reception DSP. Particularly, we separated the two PolMux channels with minimal penalty for 32 Gb/s PolMux multiCAP DSB modulation.

In this work, we demonstrate an automatic simplified and low-cost 100 Gb/s PolMux heterodyne receiver capable of working effectively with any input polarization orientation of the PolMux channels relative to the receiver. Although the configuration of the simplified receiver is based on the optical scheme outlined in our previous works, the key distinction of this work is the development of a new DSP able to automatically recover the two PolMux channels without supervision, regardless of the input state of polarization of the signal. As in our previous works, we use multiCAP signals to increase the bit count and OSSB modulation to maintain an electrical 11.25 GHz bandwidth in a heterodyne scheme, thus enabling the use of 10G electronics at both the transmitter and receiver ends. Although coherent receivers are capable of managing phase-related penalties through DSP, OSSB modulation additionally avoids power fading issues without requiring further digital processing. A sensitivity of −29 dBm, when both channels are active, has been measured for the receiver supporting 100 Gb/s transmission, and −38.7 dBm for 50 Gb/s. To the best of our knowledge, this is the first demonstration of a 100 Gb/s/λ PolMux heterodyne coherent receiver supporting any input polarization.

In Section 2, we will present the architecture of the PolMux receiver. Section 3 will describe the experimental setup, and Section 4 will detail the obtained results. These results are discussed in Section 5. Finally, Section 6 will summarize the conclusions of the research presented.

2. POLMUX HETERODYNE RECEIVER ARCHITECTURE

A. Glance Polarization Independent Coherent Optical Receiver

Our PolMux heterodyne coherent receiver, that can be seen in Fig. 1, is based on the polarization insensitive coherent receiver proposed by Glance [12]. Our receiver employs a similar optical stage to Glance's: a polarization maintaining (PM) coupler, followed by a polarization beam splitter (PBS) and two photodetectors (PD). The state of polarization of the LO is fixed at 45° with respect to the PBS axis and is shifted from the central wavelength of the received signal. This receiver architecture endures a sensitivity penalty of 3 dB compared to classical polarization controlled heterodyne receivers, such as those used in [18,19]. However, it achieves polarization insensitivity by simply adding both detected signals. In our receiver, these two detected signals are digitalized and digitally processed to recover the PolMux information.

B. Receiver Digital Signal Processing

Receiver digital signal processing (Rx-DSP), illustrated in Fig. 1, is the core of the simplified PolMux receiver, transforming the two digitalized PD signals into the original PolMux transmitted symbols. Initially, the DSP down-converts both signals using a PLL locked to the beat frequency between the LO and the residual optical carrier of one of the PD signals. Then, orthogonal multiCAP filters are applied for each multiCAP band, and the received IQ symbols are sampled and enhanced by a phase correction algorithm. In our system the PLL is crucial because, as it will be shown later, the multiCAP bands are not only frequency-shifted but are also inverted compared to their frequency order in transmission. The PLL implementation is based on a modification of the classical Costas loop [20] commonly used with PSK modulations. The PLL automatically locks to the strongest carrier presented in the PD signals.

The received IQ symbols represent a mixture of the original transmitted PolMux XY symbols, primarily due to misalignment with the PBS axis in the receiver caused by polarization rotation throughout the transmission system. To recover the original PolMux XY symbols, we employ a linear combination of the received IQ symbols using a four complex coefficients

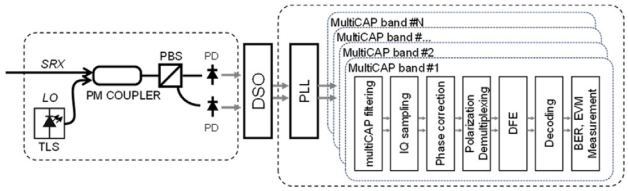

Fig. 1. Architecture of the proposed digital-PolMux heterodyne receiver.

matrix. This matrix is designed to invert the polarization rotation in the system diverging from the conventional approach of using four finite-impulse-response (FIR) filters structured in a two-by-two butterfly configuration [21]. These FIR filters are employed to equalize and monitor all the polarization rotations and impairments [22,23], a process that is essential but computationally demanding, especially in high-bandwidth and long-reach PolMux transmissions [24]. In contrast, our proposed simplified polarization demultiplexing matrix significantly reduces computational complexity without notable impact due to the narrow bandwidth used for our multiband modulation where a nearly constant response of the fiber can be assumed. For each polarization and multiCAP band, these four complex coefficients are determined by least square error using a sequence of known symbols.

Once the XY symbols are demultiplexed, they are equalized by a decision feedback equalizer (DFE) to compensate intersymbol interference (ISI) caused by the non-flat response of the opto-electrical components in the transmitter and receiver. Subsequently, the error vector magnitude (EVM) and the bit error rate (BER) are calculated from these equalized symbols.

C. multiCAP OSSB Modulation

Carrierless amplitude and phase (CAP) modulation transmits data over two orthogonal components, namely, the in-phase (I) and quadrature (Q) components as in quadrature amplitude modulation (QAM). This is achieved using two orthogonal filters [25], thereby avoiding the use of carriers or oscillators and, therefore, reducing the inherent transmitter and receiver synchronization complexity compared to QAM. The impulse responses of the CAP filters result from multiplying two orthogonal sinusoidal waveforms with a pulse shaper filter, typically a square root raised cosine (SRRC), although other spectrally efficient filters may also be employed [26].

In multiCAP, the transmission spectrum is sliced into several bands, enabling the correction of non-flat channel response and achieving higher spectral efficiencies than single-band CAP, especially in very distorted channels. MultiCAP bands are generated using several pairs of orthogonal filters, similar to standard CAP, but with different central frequencies [27], as depicted in Fig. 2. It is noteworthy that multiCAP supports variable symbol-rates and power levels in each band, features that are particularly beneficial in non-symmetric downstream scenarios and in non-flat frequency response channels. Specifically, multiCAP has been selected for this work to maximize the use of the limited bandwidth of the PDs by using power loading in the higher frequency bands.

At the reception stage, the received signal is filtered with a pair of matched filters for each multiCAP band, extracting the signals and the received IQ symbols.

When a real baseband signal is used to modulate a carrier, two identical bands appear on each side of the carrier in the frequency domain, obtaining a double-side-band (DSB) modulation that contains redundant information. Single side band (SSB) modulation takes advantage of this by reducing the occupied bandwidth, suppressing one of the two identical bands in the DSB. There exist different methods for generating an OSSB signal, with the use of arbitrary waveform generators

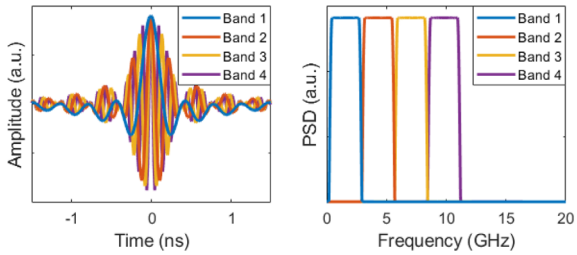

Fig. 2. Impulse response (left) and spectra (right) of the orthogonal filters used in a 10 Gbd multiCAP with four bands at 2.5 Gbd each band.

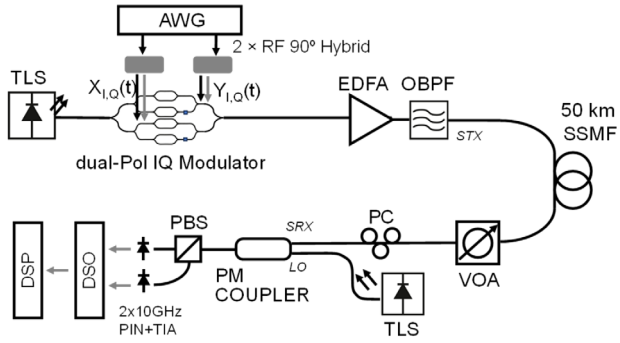

Fig. 3. Experimental setup.

(AWGs), digital Hilbert transform, and IQ optical modulators being among the most common techniques. In this work, we reduce these requirements by employing a pair of RF 90° hybrids to obtain the analog Hilbert transform and drive the in-phase and quadrature components of an IQ modulator [28]. The result is an OSSB-multiCAP signal with half the bandwidth of the original DSB-multiCAP signal. Reducing the optical bandwidth occupied would facilitate the integration of additional channels or users in an ultra-DWDM scenario.

3. EXPERIMENTAL SETUP

Figure 3 shows the experimental setup used to evaluate the performance of the downstream and the PolMux coherent receiver.

A. Transmitter

The first step in the digital transmitter corresponds to the mapping of different pseudo random binary sequence (PRBS) data streams into QAM symbols for each multiCAP band. Then, the mapped symbols are up-sampled and filtered with the corresponding orthogonal filters of each multiCAP band. Finally, these components are combined to generate the modulation signal for one polarization; the process is repeated to obtain the signal for the other polarization. Depending on the desired aggregated data-rate, we use either 4 or 5 multiCAP bands and a different constellation order: 4 × 2.5 Gbd bands at 4-QAM will be used for each polarization to obtain a 40 Gb/s bitrate, 16-QAM for 80 Gb/s and 32-QAM for 100 Gb/s, while 5 × 2.5 Gbd bands at 4-QAM will be used for 50 Gb/s. The bands have been configured to have the same performance

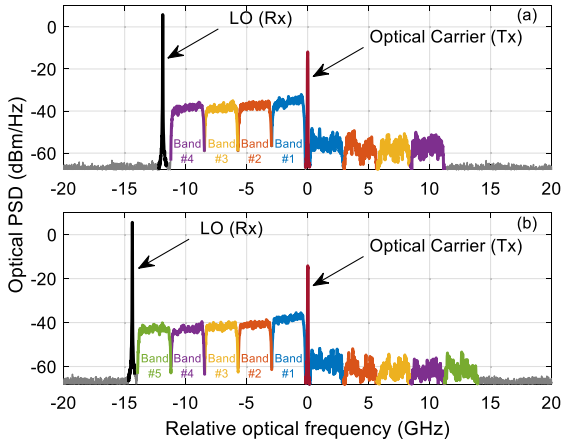

Fig. 4. High resolution optical power spectral density of the transmitted signals for 40/80/100 Gb/s (a) and 50 Gb/s (b) and the receiver local oscillator (LO).

in terms of data-rate and BER; therefore, the optical power loading capability of MultiCAP has been used to compensate the spectral response of the system. The multiCAP orthogonal filters employ a SRRC pulse shaping with a roll-off factor of 0.1 and a length of 100 symbols. These values represent a balanced trade-off between complexity and performance. Lower roll-off factors and/or higher lengths would enhance the performance but would also increase the cost and complexity of the digital signal processing.

The electrical signals of the digital transmitter are generated using the two outputs of an 80 GSa/s AWG, with one output dedicated to each polarization. These AWG outputs are connected to two RF 90° hybrids to obtain the I and Q components for each of the signals within the PolMux, generating the OSSB modulation. These outputs are amplified and feed the four inputs of a PolMux IQ modulator biased at the null-point for both polarizations. The light source is a tunable laser source (TLS), with a linewidth lower than 100 kHz, operating at a wavelength of 1550 nm, and half of its 11 dBm emitted optical power is used to feed each of the two polarization channels.

The transmitted optical signal for both PolMux channels is an OSSB modulation, as can be seen in the high-resolution optical spectra in Fig. 4. This signal occupies 11.2 GHz for 40/80/100 Gb/s and 14.2 GHz for 50 Gb/s. Although the optical suppression ratio between the upper and lower bands is only 20 dB, it is enough to prevent interference at the receiver. As shown in the figure, there is higher optical power loading in the bands closer to the optical carrier, which corresponds to the highest frequencies at the receiver. Optical power loading is even stronger in the configuration with five bands, as the first band is going to be located far from the electrical bandwidth of the optical receiver. The OSSB modulation increases power efficiency and receiver sensitivity compared to the commonly used CAP or multiCAP signals based on intensity modulation (IM) by reducing power in the optical carrier and consequently lowering the carrier-to-signal power ratio (CSPR).

The PolMux optical signal is amplified and filtered before being injected into 50 km of standard single-mode fiber (SSMF). An optical band pass filter (OBPF) with a bandwidth of 100 GHz is used to mitigate the amplified spontaneous emission (ASE) noise from the amplification process originating in the erbium doped fiber amplifier (EDFA). The input power of the SSMF is set at +2 dBm, i.e., −1 dBm per polarization. To evaluate the performance of the system, we have included a variable optical attenuator (VOA) and a polarization controller (PC) to adjust the received power and the state of polarization (SOP) of the received signal.

B. Receiver

At the receiver end, the received PolMux signal is mixed with the LO in the polarization insensitive receiver shown in Fig. 1 using a 50/50 PM coupler. The LO is a TLS, with a linewidth lower than 100 kHz, whose state of polarization is fixed at 45° relative to the PBS axis and is shifted from the central wavelength of the received signal to use all the available bandwidth in the two PIN + TIA photodetectors. The responsivities and transimpedance gains of the PDs are 0.86 and 0.87 A/W and 520 and 513 Ω, respectively. Although a 50/50 PM coupler and 10 Gb/s receivers are used, they can be replaced with couplers of different ratios and PDs with wider bandwidths to enhance sensitivity and increase data-rates, respectively. The detected signals are digitalized by a 20 GHz digital storage oscilloscope (DSO) at 80 Gsa/s, and they are digitally processed offline as previously described.

As illustrated in Fig. 5, which displays the spectra of received signals for the four different spectral configurations, the signal exhibits a very low carrier-to-signal power ratio that enhances sensitivity by maximizing the DSO resolution. It is important to note that the multiCAP bands are mirrored in frequency with respect to the generated ones. For example, Band #1 is the lowest in frequency and closest to the optical carrier in transmission, as seen in the spectrum of Figs. 2 and 4, but it becomes the highest one in frequency upon reception, as can be seen in Fig. 5. The PLL downconverts the detected signals and it also reorders the multiCAP bands in frequency before applying the orthogonal multiCAP filters.

The PLL is locked to the tones observed at 11.5 GHz and 14.4 GHz for four and five multiCAP bands, respectively. These tones are the result of the beating between the LO and the projection of the residual optical carriers in both polarizations onto the PBS axes. Depending on the SOP of the received

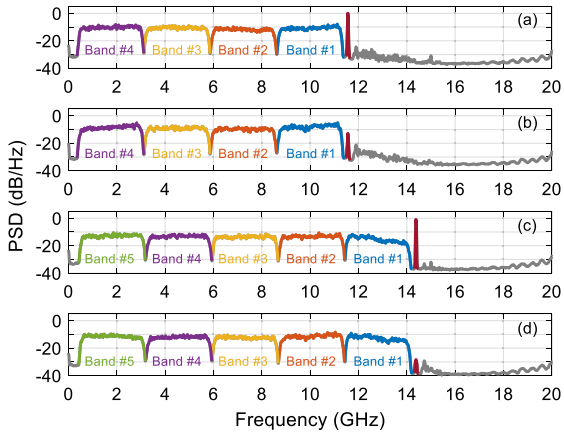

Fig. 5. Electrical power spectral density of the received signals at PD1 and PD2 (with a received optical power of −20 dBm) for 40 Gb/s (a) and (b) PD2 and 50 Gb/s (c) and (d).

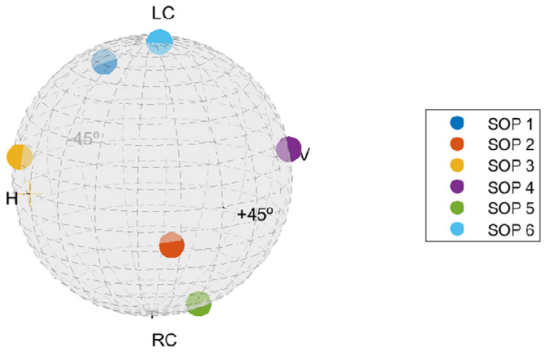

Fig. 6. Poincaré sphere representation of the receiver signal SOPs evaluated.

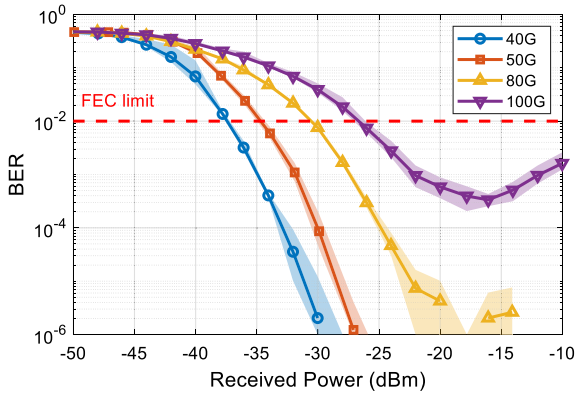

Fig. 7. BER curves for the BTB scenario as a function of the received power for 40–100 Gb/s at the hard-decision FEC limit.

signal, the projection of the carriers can generate interferences between them resulting in differences in the power of the observed tone at each PD. Taking this into account, the PLL was designed to lock automatically to the strongest carrier because this effect can be as strong as the high difference shown in the height of the tones in Figs. 5(c) and 5(d) where the residual carriers are maximum and nearly absent, respectively.

It should also be noted in Fig. 5 that the non-flat response of the photo-receivers is compensated by the aforementioned optical power loading in the higher frequency bands, resulting in almost flat received electrical spectra. However, despite the power loading, the power spectral density in the fifth multiCAP band is not entirely flat, and the electrical signal power decreases with the number of multiCAP bands for the same received optical power. These two behaviors will impact the performance of the spectral configurations, as will be demonstrated later. Additionally, the spectra notably show the suppression of the upper optical lateral band due to the limited bandwidth of the PDs.

4. RESULTS

The simplified receiver performance has been evaluated using BER measurements across various received SOPs, configured by the PC in the experimental setup, and for four different data-rates. The SOPs presented are six states uniformly distributed on the Poincaré sphere defined by the receiver PBS axis, as depicted in Fig. 6. They include the best cases (SOPs aligned with the PBS axes) and the worst cases (SOPs oriented at 45° with the PBS axes). The sensitivity of the system is determined by the received optical power at BER values of 1×10^{-2} and 2×10^{-2}, which are considered reference levels for hard–decision (HD) and soft–decision (SD) forward error correction (FEC) decoding, respectively [29,30].

A. Sensitivity Limits

Figure 7 shows the aggregated BER values for all the multiCAP bands and both polarizations, plotting them as a function of the received optical power in the back-to-back (BTB) configuration. The solid line of each data-rate represents the mean BER value of the six SOPs, while the shaded region represents the range of the measured BER values from the best to the worst SOP.

Table 1. Sensitivity Values for the Different Rates and FECs at the BTB Scenario

	40 Gb/s	50 Gb/s	80 Gb/s	100 Gb/s
HD-FEC	−37.4 dBm	−34.7 dBm	−30.4 dBm	−26.6 dBm
SD-FEC	−38.3 dBm	−35.7 dBm	−31.8 dBm	−28.2 dBm

The most remarkable result is the reduced dispersion of measured BER values for the different SOPs, indicating that our DSP effectively demultiplexes the PolMux channels independent of the incoming SOP. Sensitivity at the HD (SD) FEC BER limits, as shown in Table 1, increases with the data-rate from −37.4 dBm (−38.3 dBm) for 40 Gb/s to −26.6 dBm (−28.2 dBm) for 100 Gb/s. Contrary to expectations, the increase in sensitivity is not strictly linear with the rate, particularly for the 50 Gb/s scenario. This may be attributed to the additional multiCAP band used, which is allocated slightly out of the PDs nominal bandwidth and exhibits a clear distortion that can be seen in the electrical spectra in Fig. 5. These values result in a power budget of 28.6 dB (30.2 dB) for 100 Gb/s for any input SOP, considering the +2 dBm of transmitting power and the HD (SD) FEC limits. For the lower data-rate evaluated, 40 Gb/s, the power budget nearly reaches 40 dB, precisely 39.4 dB, for the HD FEC. Notably, at the highest data-rate of 100 Gb/s, a BER floor of 3.5×10^{-4} is observed, likely linked to the higher constellation order (32-QAM) used, which is more susceptible to noise given by the phase noise due to the linewidth of the signal and LO lasers, and the ASE of the EDFA. The observed BER floor increase for received optical power larger than −16 dBm is due to the interference of the signal-signal beating interference (SSBI) in our non-balanced photodiodes.

Regarding the performance of both channels (polarization X and Y), Fig. 8 presents disaggregated results for channels, multiCAP bands, and the SOP at 40 Gb/s, indicating that the Y-channel performs slightly worse than the X-channel, with a penalty lower than 0.5 dB. This discrepancy may be related to power imbalances during the signal generation or amplification at the transmitter. Generally, the performance of the worst channel depends on the SOP, alternating between

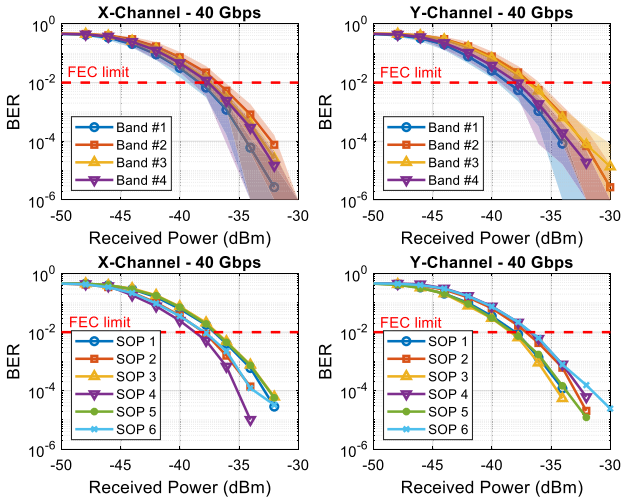

Fig. 8. BER curves for the BTB scenario as a function of the received power for 40 Gb/s at the HD FEC limit for the different multiCAP bands (uppers) and SOPs (lowers).

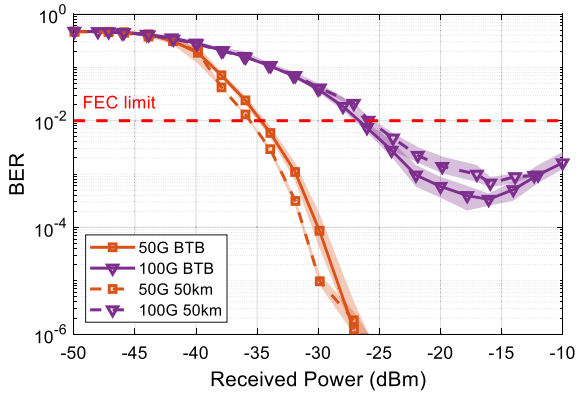

Fig. 9. BER curves for the BTB and 50 km length optical fiber scenarios as a function of the received power for 50 and 100 Gb/s at the HD FEC limit.

Table 2. Sensitivity Values for the Different Rates and FECs at the 50 km Fiber Scenario

	50 Gb/s	100 Gb/s
HD-FEC	−35.5 dBm	−25.8 dBm
SD-FEC	−36.7 dBm	−27 dBm

channels. This behavior could be associated with the PDs' different responsivities, noise factors, or imbalances in the receiver coupler.

According to Fig. 8, the worst performing multiCAP bands are the central bands, rather than those farthest from or nearest to the optical carrier, which may typically be distorted by the limited bandwidth of the RF 90° hybrids and PDs. These bands are also more susceptible to carrier and phase shifts due to mismatches in the PLL and the multiCAP orthogonal filters. In our experiments, we have compensated the BER penalties through power-loading, adjusting the power ratio favorably in the extreme bands. As a result, the power allocated in the central bands is lower, leading to slightly worse BER in these bands, possibly due to an overcompensation of the degradation.

In the fiber scenario, the sensitivity is slightly degraded by distortions and effects introduced by the 50 km fiber length. As can be seen in Fig. 9, the penalty at the 50 Gb/s rate is almost negligible compared to the BTB scenario, although a 0.6 dB penalty is observed for the 100 Gb/s scenario. More critically, there is an increase in the BER floor presented in the 100 Gb/s curve from 3.5×10^{-4} in the BTB scenario to 6.9×10^{-4} with the fiber. This floor, as previously mentioned, may be attributed to the higher constellation order used in the 100 Gb/s (32-QAM) rate and the limited transmitter OSNR, which is not able to adequately generate the constellation. Additionally, a BER floor is observed for the 80 Gb/s (16-QAM) rate, but at a lower level of approximately 2×10^{-6}, as illustrated in Fig. 7.

These sensitivities for the 50 km fiber scenario, presented in Table 2, combined with the increase of the BER value due to the saturation of the coherent receiver for received optical power higher than −8 dBm, constrain the effective power budget to a range between 27.8 dB (29 dB) and 10 dB (10 dB) for the 100 Gb/s rate and HD (SD) FEC. These results provide an available optical power range for different optical network units (ONUs) in a real PON scenario of 17.8 dB (19 dB). For the 50 Gb/s rate, the power budgets obtained are enhanced by an additional 10 dB, reaching up to 37.5 dB and 38.7 dB for the HD FEC and the SD FEC, respectively.

5. DISCUSSION

Measurements show that the combination of 10G optoelectronics, advanced modulation formats, and coherent heterodyne receivers present a viable, low-cost, and simplified alternative for 100 Gb/s receivers. The use of 25G receivers will enable reaching higher data-rates, such as 200 Gb/s, but it will also increase costs and demands on RF components. Most notably, this upgrade will require a significant boost in DSP capacity.

We have demonstrated the feasibility of PolMux transmission using heterodyne coherent receivers, with measured penalties proving to be negligible. Nonetheless, it is essential to use adaptive algorithms to obtain the demultiplexing matrix and separate the two polarization channels. This could effectively be achieved by incorporating an additional narrow multiCAP band with pilots or known training symbol sequences.

Although in the presented measurements the SOP was stable along the captured signals, based on the demonstrated performance of our DSP, we are confident in its robustness against dynamic SOP changes. The frequency of the training symbol sequence can be adjusted in order to retrain the demultiplexing algorithm and follow the polarization dynamic evolution. For a real implementation, the sequence of known symbols in the header of the frame of each multiCAP band can be combined with the additional narrow multiCAP band, commented previously. Naturally, as the dynamic SOP changing speed increases, more frequent sequences would also be required, thereby reducing the effective data-rate. Therefore, there should be a

trade-off between the scrambling speed tolerance and effective data-rate.

In the receiver DSP, the primary challenge is the requirement of PLLs to recover the baseband signals. To minimize DSP complexity, we have implemented a single PLL for both channels, enhanced by a simplified 4-coefficient demultiplexing matrix, though further optimizations are possible. Additionally, bands positioned further from the carrier may suffer increased errors due to mismatches with the PLL, and frequencies above 10G will require alternative mechanisms to keep the signals synchronized.

It is remarkable that, in this work, we have not used any signal pre-distortion at the transmitter. Implementing signal pre-distortion at the transmitter may improve the sensitivity levels and increase the emitted power by compensating nonlinear distortions in the channel. This could potentially enable reaching optical power budget values higher than 30 dB for 100 Gb/s.

The power budgets and power range values meet the requirements defined in the latest PON standards. For example, the power budgets obtained for 100 Gb/s and SD-FEC comply with the optical distribution network (ODN) optical path loss Class N1 defined in the 50G-PON standard with a minimum and maximum optical path loss of 14 dB and 29 dB, respectively [29]. On the other hand, the huge power budgets obtained in the 50 Gb/s scenario for the HD (SD) FEC of 37.5 dB (38.7 dB) comfortably exceed all the ODN class requirements defined in the 50G-PON standard.

These power budgets should be compatible with an upstream link. However, the transmission stage presented in this work is not feasible for the upstream due to the cost of the IQ modulator and the RF 90° hybrids. In a cost-effective ONU transmitter, we may reuse part of the LO optical power as a source, use an intensity modulator, and include a low sensitivity receiver, such as a quasicoherent receiver [10] at the optical line terminal (OLT). With this solution, if a 10 GHz electrical bandwidth is maintained for the modulator at the ONU, the link would not be symmetrical, which is not uncommon in PON standards.

6. CONCLUSION

We have demonstrated that a combination of advanced modulation techniques, polarization multiplexing, simplified polarization independent heterodyne coherent receiver architecture, and digital signal processing can achieve a 100 Gb/s link over 50 km using 10 GHz electrical bandwidth devices. Our proposal shows a 29 dB optical power budget for a 2×10^{-2} BER condition (SD FEC), which makes this link suitable for passive optical networks. For lower bitrates, the results are even more favorable, achieving optical power budgets of 38.7 dB for 50 Gb/s links. Moreover, we have studied the impact of changing the input state of polarization on the simplified coherent PolMux receiver, demonstrating that the developed signal processing effectively separates the PolMux channels under different polarization conditions, with minimal penalty during channel recovery.

Funding. This work was supported by the Gobierno de Aragón (T20_23R), the Agencia Estatal de Investigación MICIU/AEI/10.13039/501100011033 (PID2020-114916RB-I00), and the Agencia Estatal de Investigación MICIU/AEI/10.13039/501100011033 and European Union NextGenerationEU/PRTR (PDC2023-145803-I00).

REFERENCES

1. V. Houtsma, D. van Veen, and E. Harstead, "Recent progress on standardization of next-generation 25, 50, and 100G EPON," J. Lightwave Technol. **35**, 1228–1234 (2017).
2. Y. Zhu, L. Yi, B. Yang, *et al.*, "Comparative study of cost-effective coherent and direct detection schemes for 100 Gb/s/λ PON," J. Opt. Commun. Netw. **12**, D36–D47 (2020).
3. W. Hu and Y. Zhu, "100G and beyond for PON and short reach optical networks," in *Optical Fiber Communication Conference (OFC)* (2023), paper Th3G.5.
4. C. Ye, D. Zhang, X. Huang, *et al.*, "Demonstration of 50 Gbps IM/DD PAM4 PON over 10 GHz class optics using neural network based nonlinear equalization," in *European Conference on Optical Communication (ECOC)* (2017).
5. J. Bai, L. Li, Y. Fu, *et al.*, "Comparative investigation of Kramers-Kronig and FFE in low-cost PON with C-band SSB-PAM4 signal," in *24th OptoElectronics and Communications Conference (OECC) and International Conference on Photonics in Switching and Computing (PSC)* (2019).
6. M. I. Olmedo, T. Zuo, J. B. Jensen, *et al.*, "Multiband carrierless amplitude phase modulation for high capacity optical data links," J. Lightwave Technol. **32**, 798–804 (2014).
7. J. Zhang, M. Zhu, K. Wang, *et al.*, "The best modulation format for symmetrical single-wavelength 50-Gb/s PON at O-band: PAM, CAP or DMT?" in *Optical Fiber Communication Conference (OFC)* (2021), paper W1H.3.
8. P. Torres-Ferrera, F. Effenberger, M. S. Faruk, *et al.*, "Overview of high-speed TDM-PON beyond 50 Gbps per wavelength using digital signal processing [Invited Tutorial]," J. Opt. Commun. Netw. **14**, 982–996 (2022).
9. G. Rizzelli Martella, A. Nespola, S. Straullu, *et al.*, "Scaling laws for unamplified coherent transmission in next-generation short-reach and access networks," J. Lightwave Technol. **39**, 5805–5814 (2021).
10. J. A. Altabas, O. Gallardo, G. S. Valdecasa, *et al.*, "Roadmap for next generation optical networks based on quasi-coherent receivers," in *22nd International Conference on Transparent Optical Networks (ICTON)* (2020).
11. I. B. Kovacs, M. S. Faruk, and S. J. Savory, "Simplified coherent receivers for passive optical networks," in *49th European Conference on Optical Communications (ECOC)* (2023), pp. 1182–1185.
12. B. Glance, "Polarization independent coherent optical receiver," J. Lightwave Technol. **5**, 274–276 (1987).
13. E. Ciaramella, "Polarization-independent receivers for low-cost coherent OOK systems," IEEE Photonics Technol. Lett. **26**, 548–551 (2014).
14. M. S. Erkılınç, D. Lavery, K. Shi, *et al.*, "Polarization-insensitive single-balanced photodiode coherent receiver for long-reach WDM-PONs," J. Lightwave Technol. **34**, 2034–2041 (2016).
15. M. Barrio, D. Izquierdo, J. A. Altabás, *et al.*, "50 Gb/s transmission using OSSB-MultiCAP modulation and a polarization independent coherent receiver for next-generation passive optical access networks," J. Lightwave Technol. **39**, 5722–5729 (2021).
16. M. Barrio, D. Izquierdo, J. Cerdá, *et al.*, "Spectrally efficient downstream 100 Gb/s PolMux multi-CAP OSSB transmission and coherent reception using 10G electronics for passive optical networks," in *Optical Fiber Communication Conference (OFC)* (2021), paper F2H.3.
17. M. Barrio, D. Izquierdo, P. Sevillano, *et al.*, "PolMux reception using a low-cost heterodyne receiver for coherent PONs," in *Conference on Lasers and Electro-Optics (CLEO)* (2023).
18. D. Izquierdo, J. A. Altabas, J. Clemente, *et al.*, "Flexible resource provisioning of coherent PONs based on non-orthogonal multiple access and CAP signals," in *45th European Conference on Optical Communication (ECOC)* (2019).

19. D. Izquierdo, J. A. Altabas, M. Barrio, *et al.*, "Flexible resource provisioning of polarization independent coherent PONs based on non-orthogonal multiple access and multiCAP modulation," J. Opt. Commun. Netw. **13**, 140–146 (2021).
20. J. P. Costas, "Synchronous communications," Proc. IRE **44**, 1713–1718 (1956).
21. S. J. Savory, "Digital filters for coherent optical receivers," Opt. Express **16**, 804–817 (2008).
22. K. Kikuchi, "Fundamentals of coherent optical fiber communications," J. Lightwave Technol. **34**, 157–179 (2016).
23. M. S. Faruk, Y. Mori, C. Zhang, *et al.*, "Multi-impairment monitoring from adaptive finite-impulse-response filters in a digital coherent receiver," Opt. Express **18**, 26929–26936 (2010).
24. C. R. S. Fludger, T. Duthel, D. van den Borne, *et al.*, "Coherent equalization and POLMUX-RZ-DQPSK for robust 100-GE transmission," J. Lightwave Technol. **26**, 64–72 (2008).
25. A. F. Shalash and K. K. Parhi, "Multidimensional carrierless AM/PM systems for digital subscriber loops," IEEE Trans. Commun. **47**, 1655–1667 (1999).
26. P. A. Haigh, P. Chvojka, S. Zvánovec, *et al.*, "Analysis of Nyquist pulse shapes for carrierless amplitude and phase modulation in visible light communications," J. Lightwave Technol. **36**, 5023–5029 (2018).
27. J. Wei, Q. Cheng, D. G. Cunningham, *et al.*, "100-Gb/s hybrid multi-band CAP/QAM signal transmission over a single wavelength," J. Lightwave Technol. **33**, 415–423 (2015).
28. Y. Zeng, Z. Dong, Y. Chen, *et al.*, "A novel CAP-WDM-PON employing multi-band DFT-spread DMT signals based on optical Hilbert-transformed SSB modulation," IEEE Access **7**, 29397–29404 (2019).
29. "50-gigabit-capable passive optical networks (50G-PON): physical media dependent (PMD) layer specification," ITU-T Recommendation G.9804.3 (2021).
30. R. Borkowski, Y. Lefevre, A. Mahadevan, *et al.*, "FLCS-PON—an opportunistic 100 Gbit/s flexible PON prototype with probabilistic shaping and soft-input FEC: operator trial and ODN case studies," J. Opt. Commun. Netw. **14**, C82–C91 (2022).